A NOVEL JOINT RADAR AND COMMUNICATION SYSTEM BASED ON RANDOMIZED PARTITION OF ANTENNA ARRAY

Dingyou Ma, Tianyao Huang, Yimin Liu⋆, Xiqin Wang

Department of Electronic Engineering, Tsinghua University, Beijing, China

ABSTRACT

Partitioning the antenna array into different subarrays is a flexible scheme in the joint radar and communication system. However, the traditional fixed partition of the antenna array cannot make full use of the complete aperture. In this paper, we propose a novel antenna partition scheme. In this scheme, the antenna is randomly and dynamically chosen as radar or communication unit. The dynamic randomness introduces extra channel capacity of the communication system, and enables the radar system approximately obtain the resolution and sidelobe level of a full antenna array simultaneously. The channel capacity, Cramér Rao Bound and the ambiguity function are theoretically analyzed. Pareto Front is used to demonstrate the performance improvement of the proposed system over the traditional fixed partition system.

Index Terms— Joint radar and communication system, randomized switched antenna array, channel capacity, Cramér Rao Bound, generalised spatial modulation

1. INTRODUCTION

Radar and communication both are significant functions in many applications, such as intelligent transportation, remote sensing and electronic warfare. Recent years, the hardware and the frequency spectrum in radar and wireless communication have become more and more similar[1]. Joint design of the radar and communication system saves hardware resource, lowers the cost and reduces the system volume. Hence, the joint design of radar and communication has attracted great attentions.

Many schemes have been proposed on joint radar and communication system (JRACS), which include joint waveform design[1], space multiplexing scheme[2], time sharing scheme[3] and so on. Either scheme has its advantages and disadvantages. In program AMRFC[4], a common set of broad-band antenna array is partitioned into many subarrays for different functions. In that scheme, both subsystems can work simultaneously. The transmitting power, the transmitting and receiving antennas are all flexible for system design. However, the fixed partition of the antenna array can not make full use of the complete antenna aperture. The resolution of radar and the capacity of the communication system can be improved if the full aperture is used.

Recent years, a new communication modulation scheme, named generalised spatial modulation (GSM)[5, 6] was proposed. In this system, the spatial bits are conveyed in the activated combination of the transmit antennas, which increases the channel capacity. While in radar system, a kind of randomized switched antenna array (RSAA)[7] can approximately achieves the performance of the full antenna array using only a part units of the antenna array.

This work is supported by the National Natural Science Foundation of China (Grant No. 61571260).

Inspired by the similar character of GSM and RSAA, we propose a novel antenna partition scheme for the design of JRACS in this paper. In this scheme, the communication transmitter and the radar receiver share the same antenna array. The antenna units are randomly and dynamically chosen working for radar or communication. At each communication transmitting time, some antennas are randomly selected as communication units from the antenna array and the rest are used by radar. This new system improves the channel capacity of the communication subsystem and achieves the high resolution and low sidelobe level as the full antenna array.

The rest of the paper is organized as follows. In section 2, the system model and the signal model is proposed. In section 3, the performance metrics of radar and communication system are presented and analyzed. In section 4, the performance of the proposed system is compared with the comparison system using the Pareto Front. Section 5 is the conclusion.

2. SYSTEM MODEL

The system sketch of the proposed system is depicted in Fig.1. In this system communication transmitter and radar receiver share the same uniform linear array (ULA) with M units and a constant interelement distance d. The radar uses a separate transmitter, which is not drawn in the sketch. In this antenna array, the original point is selected as the position of the first element. Each element is connected with a transmitter and a receiver. The transmitter is used for transmitting communication waveforms, while the receiver is used for receiving radar echoes.

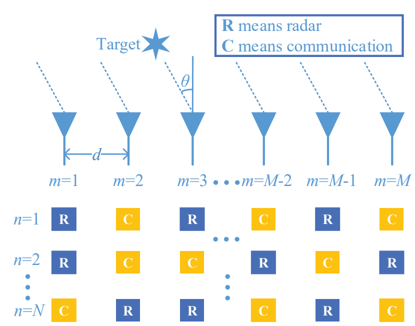

Fig. 1. The joint radar and communication system model

In the proposed system, the antenna array is randomly and dynamically chosen as radar or communication units. Specifically, at each communication transmitting time, N_a antennas are randomly selected as communication units from the M antennas according to the communication data stream, and the other $M - N_a$ antennas are used by radar.

Both radar and communication subsystems will be introduced in detail in the next subsections.

2.1. Communication subsystem

The communication subsystem which randomly selects transmit antennas can be regarded as a GSM system. In a GSM system, the block of information bits are divided into constellation bits and spatial bits. The spatial bits determine the combination of transmit antennas actived at each instance[5, 8], which increases the channel capacity and improves the spectral efficiency.

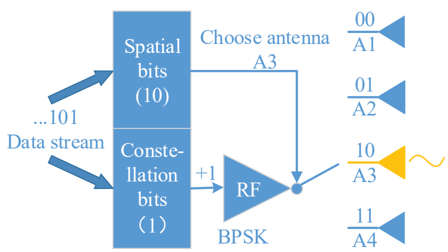

Fig. 2. Communication subsystem model

An example of the subsystem is shown in Fig.2. There are $M = 4$ transmit antennas in total, and $N_a = 1$ antenna is active at each instance. The number of antenna combinations is $K = 2^s$, where s is $\lfloor \log_2 \binom{M}{N_a} \rfloor$ and $\lfloor \cdot \rfloor$ is the floor operation[5]. If a Q-order amplitude phase modulation (APM) is chosen, each active antenna can convey $\log_2 Q$ bits. Consequently, at each transmitting time, $N_a \log_2 Q + s$ bits can be transmitted. In Fig.2, the APM is Binary Phase Shift Keying (BPSK). The information block 101 is mapped to activate the antenna A3, and the transmitting symbol is $+1$.

2.2. Radar subsystem

The radar coherent processing interval (CPI) consists of N pulses. A space-time snapshot $\mathbf{y} \in \mathbb{C}^{NL}$ refers to a vector of the samples corresponding to the same range gate[9, 10], where L is $M - N_a$. The received signal $\mathbf{y}$ can be expressed as

$$\mathbf{y} = \mathbf{r} + \mathbf{w}, \tag{1}$$

where $\mathbf{w} \in \mathbb{C}^{NL}$ is an additive noise vector. The vector $\mathbf{r}$ is composed of N vectors, $\mathbf{r} = [\mathbf{s}_1^{\mathrm{T}}, \mathbf{s}_2^{\mathrm{T}}, \cdots, \mathbf{s}_N^{\mathrm{T}}]^{\mathrm{T}} \in \mathbb{C}^{NL}$, where $\mathbf{s}_n \in \mathbb{C}^L$ is received from L receiving antennas during the nth pulse.

If there exists an ideal point target with direction θ, relative radial velocity v and initial range r. The lth entry of $\mathbf{s}_n$ is

$$s_n(l) = Ae^{j\phi - j\frac{4\pi f_c v n T}{c} + j\frac{2\pi f_c d[X(n,l)-1]\sin\theta}{c}}, \tag{2}$$

where $X(n, l)$ is the index of the lth receiving antenna in the antenna array during the nth pulse, T is the pulse repetition interval, f_c is the carrier frequency, c is the light speed, and $Ae^{j\phi}$ is the complex amplitude of the echo.

3. PERFORMANCE METRICS

In this section, performance metrics will be proposed and analyzed. Channel capacity is utilized to evaluate performance of the communication subsystem. Ambiguity function is utilized to evaluate performance of the radar resolution and sidelobe effects. A narrow mainlobe of the ambiguity function implies a high resolution. In a multi-target scenario, weak targets can be masked by the sidelobes of strong targets. The grating lobes will cause ambiguity. Hence, one may hope the ambiguity function of the proposed system has a narrow mainlobe, low sidelobe and has no grating lobes. Cramér Rao Bound (CRB) is the lower bound for the mean square error (MSE) of the unbiased estimate, and can be utilized to evaluate the performance of the estimation accuracy.

3.1. Channel Capacity

The channel capacity of GSM system is the sum of the constellation capacity C_{APM} and the spatial capacity $C_{spatial}$

$$C = C_{APM} + C_{spatial}. \tag{3}$$

In (3), C_{APM} is equivalent to the capacity in a traditional Multiple Input Multiple Output (MIMO) system. Hence, with the same channel state, the capacity of a GSM system is $C_{spatial}$ bits more than that of a traditional MIMO system. Define $\mathrm{SNR_c}$ as the signal to noise ratio in the communication system. At high $\mathrm{SNR_c}$, $C_{spatial}$ is approximately $\lfloor \log_2 \binom{N_t}{N_a} \rfloor$[8] and C_{APM} is approximately $N_a \log_2 \left(1 + \frac{\mathrm{SNR_c}}{N_a}\right)$ [11].

3.2. Cramér Rao Bound

In the radar signal model (2), A, ϕ, θ and v are unknown. Define $\boldsymbol{\xi} = [A, \phi, \theta, v]^{\mathrm{T}}$ as the parameter vector, and $\hat{\boldsymbol{\xi}}$ as the unbiased estimate of $\boldsymbol{\xi}$. The mean square errors (MSEs) matrix of $\hat{\boldsymbol{\xi}}$ satisfies the information inequality

$$\mathbf{E}\left\{\left(\hat{\boldsymbol{\xi}} - \boldsymbol{\xi}\right)\left(\hat{\boldsymbol{\xi}} - \boldsymbol{\xi}\right)^{\mathrm{H}}\right\} \succeq \mathbf{J}^{-1}, \tag{4}$$

where $\mathbf{J}$ is the Fisher information matrix of $\boldsymbol{\xi}$. $\mathrm{CRB}_{\hat{\xi}_i}$ is the Cramér Rao Bound of the ith entry in $\boldsymbol{\xi}$ and is equal to $[\mathbf{J}^{-1}]_{ii}$. $\mathbf{J}$ can be calculated as follows. Denote $l(\boldsymbol{r}; \boldsymbol{\xi})$ as the logarithmic likelihood function,

$$l(\boldsymbol{r}; \boldsymbol{\xi}) = C_{const} - \frac{1}{\sigma_w^2}\|\mathbf{y} - \mathbf{r}\|_2^2, \tag{5}$$

where C_{const} is a constant and σ_w^2 is the variance of each sample of the white gaussian noise $\mathbf{w}(n)$.

According to [12], the entry of $\mathbf{J}$ is

$$[\mathbf{J}]_{ij} = E\left\{\frac{\partial^2 l}{\partial \xi_i \partial \xi_j}\right\}. \tag{6}$$

In this paper, we mainly focus on the partitioning of the antenna array. After calculation, we find that the CRB of A, ϕ and v are independent of the indices of the receiving antennas. Hence, we only give the CRB of θ,

$$\mathrm{CRB}_{\hat{\theta}} = \frac{[\mathbf{J}]_{22}}{[\mathbf{J}]_{22}[\mathbf{J}]_{33} - [\mathbf{J}]_{23}[\mathbf{J}]_{32}}, \tag{7}$$

where

$$[\mathbf{J}]_{22} = \frac{2NLA^2}{\sigma^2}, \tag{8a}$$

$$[\mathbf{J}]_{33} = \frac{8\pi^2 A^2 d^2 f_c^2 \cos^2\theta}{\sigma_w^2 c^2} \sum_{n=1}^{N} \sum_{l=1}^{L} [X(n,l) - 1]^2, \tag{8b}$$

$$[\mathbf{J}]_{23} = [\mathbf{J}]_{32} = \frac{4\pi A^2 d f_c \cos\theta}{\sigma_w^2 c} \sum_{n=1}^{N} \sum_{l=1}^{L} [X(n,l) - 1]. \tag{8c}$$

3.3. Ambiguity Function

The velocity-direction ambiguity function is defined as the correlation of the transmit signal $\mathbf{r}_t$ and the received signal $\mathbf{r}_r$. The entry of the transmit signal vector can also be derived from (2) with parameter v and θ equaling zero. The received signal is from the point target with parameter $\{\Delta v, \Delta\omega\}$, where ω denotes $\sin\theta$. The amplitude of $\mathbf{r}_t$ and $\mathbf{r}_r$ are normalized. According to (1) and (2), the expression of the ambiguity function is

$$\begin{aligned} &\chi(\Delta v, \Delta\omega) = \mathbf{r}_t^{\mathrm{H}} \cdot \mathbf{r}_r \\ &= \sum_{n=1}^{N}\sum_{l=1}^{L} e^{-j2\pi(n-1)T\Delta\eta} \cdot e^{j2\pi[X(n,l)-1]d\Delta\omega/\lambda} \\ &= \chi(\Delta\eta, \Delta\omega) \end{aligned} \quad , \tag{9}$$

where $\Delta\eta = 2\Delta v/\lambda$, and $\lambda = c/f_c$.

Fig.3(a) shows the normalized ambiguity function of the proposed system. The ambiguity function has a noise-like floor. In (9), it is shown that the ambiguity function can be regarded as a stochastic process. In the rest of this section, the statistical characteristics will be analyzed. Detailed calculations are not included and will be present later in a journal version.

During the nth radar receiving pulse, the indices of the radar receiving antennas compose a random vector

$$\mathbf{X}_n = [X(n,1), X(n,2), \cdots, X(n,L)]^{\mathrm{T}} \in \mathbb{N}^L, \tag{10}$$

where $X(n,1) < X(n,2) < \cdots < X(n,L)$. Define Ω as a set composed of $\binom{M}{L}$ possible values of $\mathbf{X}_n$. The following conclusions are drawn with the assumption that $\mathbf{X}_n$ is i.i.d. with a uniform distribution $\mathrm{U}(\Omega)$.

3.3.1. Expectation

The expectation of the ambiguity function is

$$\begin{aligned} &V_1(\Delta\eta, \Delta\omega) = \mathbf{E}\{\chi(\Delta\eta, \Delta\omega)\} \\ &= \frac{L}{M} e^{-j\pi(N-1)T\Delta\eta + j\frac{\pi(M-1)d\Delta\omega}{\lambda}} \frac{\sin(N\pi T\Delta\eta)}{\sin(\pi T\Delta\eta)} \frac{\sin(M\pi d\Delta\omega/\lambda)}{\sin(\pi d\Delta\omega/\lambda)}. \end{aligned} \tag{11}$$

The normalized expectation of the ambiguity function is shown in Fig.3(b), where $f_s = 1/T$. According to (11), the mean of the ambiguity function of this system is the same as the counter part of the full element array except the amplitude. Hence, the resolution of the proposed system is approximately the same as the resolution of the full array.

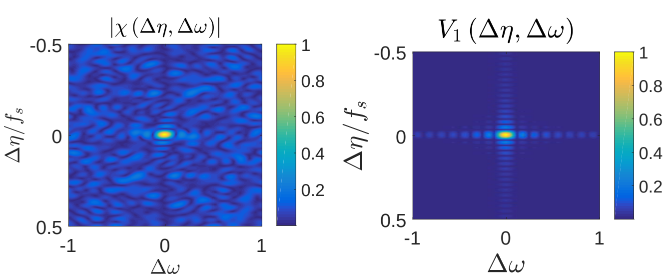

(a) Ambiguity function (b) Expectation

Fig. 3. Ambiguity function and its expectation

3.3.2. Variance

As is shown in Fig.3(a), a noise-like floor exists in the ambiguity function. In multi-target scenarios, the noise-like floor generated by strong targets may mask the weak targets. Hence it is necessary to analyze the level of this noise-like floor.

We use the variance of the ambiguity function to evaluate the value of the noise-like floor. Define the normalized variance of the ambiguity function as

$$\begin{aligned} &G(\Delta\eta, \Delta\omega) = \sigma^2(\Delta\eta, \Delta\omega)/|V_1(0,0)|^2 \\ &= \frac{L-M}{NLM^2(M-1)} \left| \frac{\sin(M\pi d\Delta\omega/\lambda)}{\sin(\pi d\Delta\omega/\lambda)} \right|^2 + \frac{M-L}{NL(M-1)}. \end{aligned} \tag{12}$$

$G(\Delta\eta, \Delta\omega)$ is shown in Fig.4(a). According to (12), the variance depends on the snapshot number N, the number of antennas used for radar L, and the direction of the target.

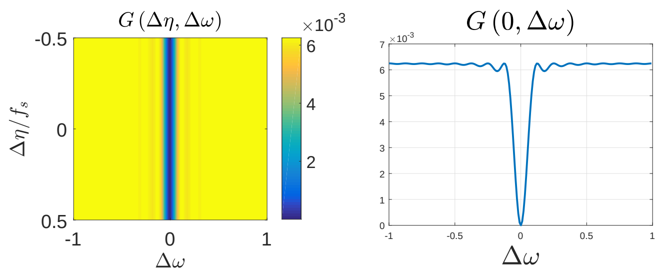

(a) Normalized variance (b) Profile of $G(0, \Delta\omega)$

Fig. 4. Normalized variance and the profile of normalized variance along $\Delta\eta/f_s$

Equation (12) also implies that:

1) The noise-like floor is a function of $\Delta\omega$, and different velocities with the same direction have the same noise-like floor.

2) The noise-like floor is inversely proportional to N. The weak target is less likely to be masked while N increases. When $\Delta\omega$ is large enough, the variance is mainly determined by the second item, as the first item will be sufficiently small. As is shown in Fig.4(b).

3.3.3. Sidelobe Level

If the sidelobe level is high, the weak targets may be masked by the sidelobe of strong targets. Hence, to detect weak targets the sidelobe is required to be less than a value. As the ambiguity function of the proposed system is a random process, one may calculate the probability of the sidelobe less than a predefined value. However, the distribution of the ambiguity function is difficult to derive. Instead, the asymptotic distribution can be used as an approximation when N is large enough. Some of the derivations are inspired by [13] and [14].

According to (9), the ambiguity function $\chi(\Delta\eta, \Delta\omega)$ can be regarded as a sum of N independent random variables $\chi_n(\Delta\eta, \Delta\omega)$, where

$$\chi_n(\Delta\eta, \Delta\omega) = \sum_{l=1}^{L} e^{-j2\pi(n-1)T\Delta\eta} \cdot e^{j\frac{2\pi[X(n,l)-1]d\Delta\omega}{\lambda}}, \tag{13}$$

and $\chi(\Delta\eta, \Delta\omega) = \sum_{n=1}^{N} \chi_n(\Delta\eta, \Delta\omega)$.

Define vector $\boldsymbol{\beta}(\Delta\eta, \Delta\omega) = [\chi_r(\Delta\eta, \Delta\omega), \chi_i(\Delta\eta, \Delta\omega)]^{\mathrm{T}}$ and $\boldsymbol{\beta}_n(\Delta\eta, \Delta\omega) = [\chi_{nr}(\Delta\eta, \Delta\omega), \chi_{ni}(\Delta\eta, \Delta\omega)]^{\mathrm{T}}$, where

$\chi_r(\Delta\eta, \Delta\omega)$ and $\chi_i(\Delta\eta, \Delta\omega)$ are the real and imaginary part of $\chi(\Delta\eta, \Delta\omega)$, and $\chi_{nr}(\Delta\eta, \Delta\omega)$, $\chi_{ni}(\Delta\eta, \Delta\omega)$ are the real and imaginary part of $\chi_n(\Delta\eta, \Delta\omega)$, respectively.

It can be validated that $\boldsymbol{\beta}(\Delta\eta, \Delta\omega)$ satisfies the sufficient condition of the Multivariate Central limit theorem [15], and thus we have the following theorem.

Theorem 1 *Random variable* $\frac{\left(\boldsymbol{\beta}(\Delta\eta,\Delta\omega)-\sum_{n=1}^{N}\mathbf{E}\{\boldsymbol{\beta}_n(\Delta\eta,\Delta\omega)\}\right)}{\sqrt{N}}$ *converges to normal distribution with mean zero and dispersion matrix* $\boldsymbol{\Sigma}$*, as* $N \to \infty$*. The dispersion matrix*

$$\boldsymbol{\Sigma} = \begin{bmatrix} \sigma_r^2(\Delta\eta, \Delta\omega) & 0 \\ 0 & \sigma_i^2(\Delta\eta, \Delta\omega) \end{bmatrix}, \tag{14}$$

where

$$\begin{aligned} &\sigma^2(\Delta\eta, \Delta\omega) = \sigma_r^2(\Delta\eta, \Delta\omega) = \sigma_i^2(\Delta\eta, \Delta\omega) \\ &= \frac{1}{2}\left[\frac{L^2 - ML}{M^2(M-1)} \cdot \left|\frac{\sin(M\pi d\Delta\omega/\lambda)}{\sin(\pi d\Delta\omega/\lambda)}\right|^2 + \frac{L(M-L)}{M-1}\right]. \end{aligned} \tag{15}$$

Define the peaklobe to sidelobe ratio as

$$\mathrm{PSLR}(\Delta\eta, \Delta\omega) = \frac{|V_1(0,0)|}{|\chi(\Delta\eta, \Delta\omega)|}. \tag{16}$$

The probability of $\mathrm{PSLR}(\Delta\eta, \Delta\omega)$ larger than r can be calculated as

$$\Pr(\mathrm{PSLR}(\Delta\eta, \Delta\omega) > r) = 1 - Q_1\left(\sqrt{\alpha}, \sqrt{x}\right), \tag{17}$$

where $Q_1(a, b)$ is the first-order Marcum Q function and $x = \frac{V_1^2(0,0)}{r^2\sigma^2(\Delta\eta,\Delta\omega)}$, and $\alpha = \frac{\mathbf{E}^2\{\chi_r(\Delta\eta,\Delta\omega)\}+\mathbf{E}^2\{\chi_i(\Delta\eta,\Delta\omega)\}}{\sigma^2(\Delta\eta,\Delta\omega)}$.

4. PERFORMANCE COMPARISON AND NUMERICAL SIMULATION

In this section, numerical simulations are utilized to verify the performance of the proposed system. In the simulations, it is set that M is 16, N is 32, the carrier frequency f_c is 9GHz, d is $\lambda/2$, T is 100μs, the target is 3km away from the antenna array, v is $100\mathrm{m/s}$, and θ is $60°$. The signal to noise ratio of radar $\mathrm{SNR_r} = 10\mathrm{dB}$, and $\mathrm{SNR_c}$ is 20dB. The amplitude of the the radar echo is normalized.

The performance improvement is demonstrated by comparing with the comparison system, where the antenna array is partitioned statically into two subarrays. There are $2^M - 2$ kinds of combinations for the division of antenna array.

Three aforementioned performance metrics are used to evaluate the system performance. The performance of the system is compared in the following steps.

First, the feasible antenna combination is chosen according to the sidelobe level. For the proposed system, the minimum PSLR corresponding to the feasible antenna combination is required to be larger than $r = 10\mathrm{dB}$ with a probability no less than $p = 90\%$. The feasible antenna combinations are found through simulation. In the simulation, L increases from 1 to $M-1$. 10000 Monte Carlo trials are performed for each L. The minimum of PSLR of each trial is calculated. The feasible antenna combinations are selected by judging whether the probability of the minimum PSLR larger than r is larger than p in the 10000 trials. For the comparison system, the ambiguity function is determinate. Hence, we can directly judge whether the minimum PSLR of the corresponding ambiguity function is larger than r. If it is larger than r, this antenna combination is feasible.

How to further choose antenna combinations from the feasible ones can be regarded as a multi-objective optimization problem (MOOP). The objects are to minimize $\mathrm{CRB}_{\hat{\theta}}$ and to maximize the channel capacity. In an MOOP, a solution is called Pareto optimal if none of the objective functions can be improved in value without degrading other objective values. The Pareto Front is the set of all the Pareto optimal solutions[16]. The Pareto Fronts of the proposed system and the comparison system are compared to show the performance improvement of the proposed system. Channel capacity and $\mathrm{CRB}_{\hat{\theta}}$ are calculated according to (3) and (7).

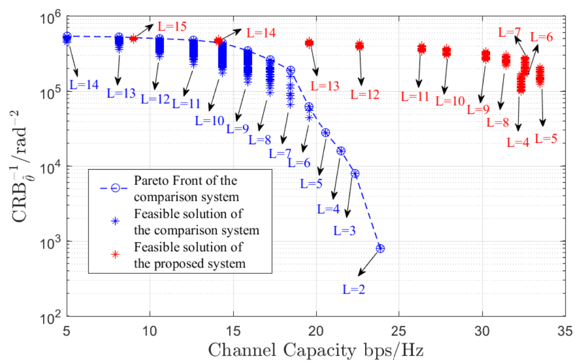

Fig. 5. Performance comparison

The channel capacity and $\mathrm{CRB}_{\hat{\theta}}^{-1}$ of all the feasible combinations are shown in Fig.5. The red asterisks and the blue asterisks represent the feasible solutions of the proposed system and the comparison system, respectively. The blue line is the Pareto Front of the comparison system. The results show that the feasible solutions of the proposed system are better than the Pareto Front of the comparison system. As the number of radar receiving antennas decreases, the $\mathrm{CRB}_{\hat{\theta}}^{-1}$ of the proposed system decreases slowly while the $\mathrm{CRB}_{\hat{\theta}}^{-1}$ of the comparison system decreases quickly. This implies that the improvement of the proposed system is significant, especially when the number of radar receiving antenna is small. Compared with the $\mathrm{CRB}_{\hat{\theta}}$ of the full antenna array, the increase of $\mathrm{CRB}_{\hat{\theta}}$ is small and the PSLR level approximately equals the PSLR of the full array. Hence, the proposed system can approximately achieve the performance of the full antenna array.

5. CONCLUSION

In this paper, we propose a novel antenna partition scheme for the design of JRACS. In this scheme, antennas are randomly and dynamically chosen as radar or communication unit. The system model and signal model of the proposed system are derived. Performance metrics, including channel capacity, CRB of the parameter estimate and ambiguity function are utilized to evaluate the performance of this new system. The asymptotic probability function of the ambiguity function are derived to approximately analyze the PSLR. The Pareto Front is used to demonstrate the performance improvement of the proposed system. The result shows that this new scheme improves the channel capacity of the communication system, meanwhile the high resolution and low sidelobe level approximately acquires the performance of a full antenna array in radar system.

6. REFERENCES

[1] Christian Sturm and Werner Wiesbeck, “Waveform design and signal processing aspects for fusion of wireless communications and radar sensing,” *Proceedings of the IEEE*, vol. 99, no. 7, pp. 1236–1259, 2011.

[2] Patrick M. Mccormick, Shannon D. Blunt, and Justin G. Metcalf, “Simultaneous radar and communications emissions from a common aperture, part i: Theory,” in *Radar Conference*, 2017, pp. 1685–1690.

[3] Zhao Wu, Yu Zhang, and Zhang Hang, “A burst sc-fde scheme for high-speed communication based on radar,” in *Military Communications Conference, Milcom 2013 -*, 2013, pp. 1541–1546.

[4] G. C. Tavik, C. L. Hilterbrick, J. B. Evins, J. J. Alter, J. G. Crnkovich, J. W. de Graaf, W. Habicht, G. P. Hrin, S. A. Lessin, D. C. Wu, and S. M. Hagewood, “The advanced multifunction rf concept,” *IEEE Transactions on Microwave Theory and Techniques*, vol. 53, no. 3, pp. 1009–1020, March 2005.

[5] A. Younis, N. Serafimovski, R. Mesleh, and H. Haas, “Generalised spatial modulation,” in *2010 Conference Record of the Forty Fourth Asilomar Conference on Signals, Systems and Computers*, Nov 2010, pp. 1498–1502.

[6] Z. An, J. Wang, J. Wang, and J. Song, “Mutual information and error probability analysis on generalized spatial modulation system,” *IEEE Transactions on Communications*, vol. 65, no. 3, pp. 1044–1060, March 2017.

[7] Chenxi Hu, Yimin Liu, Huadong Meng, and Xiqin Wang, “Randomized switched antenna array fmcw radar for automotive applications,” *IEEE Transactions on Vehicular Technology*, vol. 63, no. 8, pp. 3624–3641, 2014.

[8] Jintao Wang, Shuyun Jia, and Jian Song, “Generalised spatial modulation system with multiple active transmit antennas and low complexity detection scheme,” *IEEE Transactions on Wireless Communications*, vol. 11, no. 4, pp. 1605–1615, 2012.

[9] J. Ward, “Space-time adaptive processing for airborne radar,” in *Space-Time Adaptive Processing*, 1994, pp. 2/1–2/6.

[10] J. Ward, “Cramer-rao bounds for target angle and doppler estimation with space-time adaptive processing radar,” in *Signals, Systems and Computers, 1995. 1995 Conference Record of the Twenty-Ninth Asilomar Conference on*, 1995, pp. 1198–1202 vol.2.

[11] G. J. Foschini and M. J. Gans, “On limits of wireless communications in a fading environment when using multiple antennas,” *Wireless Personal Communications*, vol. 6, no. 3, pp. 311–335, 1998.

[12] Steven Kay, *Fundamentals of Statistical Processing, Volume I*, PTR Prentice hall, 1993.

[13] Yimin Liu, Hang Ruan, Lei Wang, and Arye Nehorai, “The random frequency diverse array: A new antenna structure for uncoupled direction-range indication in active sensing,” *IEEE Journal of Selected Topics in Signal Processing*, vol. 11, no. 2, pp. 295–308, 2017.

[14] Y Lo, “A mathematical theory of antenna arrays with randomly spaced elements,” *IEEE Transactions on Antennas and Propagation*, vol. 12, no. 3, pp. 257–268, 1964.

[15] C R Rao, “Linear statistical inference and its applications, second edition,” *Biometrics*, 1973.

[16] Yann Collette and Patrick Siarry, *Multiobjective optimization: principles and case studies*, Springer Science & Business Media, 2013.